Observation of Fermi-surface–dependent nodeless superconducting gaps in $Ba_{0.6}K_{0.4}Fe_2As_2$

A Letters Journal Exploring the Frontiers of Physics

August 2008

EPL, **83** (2008) 47001
doi: 10.1209/0295-5075/83/47001

www.epljournal.org

Observation of Fermi-surface–dependent nodeless superconducting gaps in $Ba_{0.6}K_{0.4}Fe_2As_2$

H. Ding[1(a)], P. Richard[2], K. Nakayama[3], K. Sugawara[3], T. Arakane[3], Y. Sekiba[3], A. Takayama[3], S. Souma[2], T. Sato[3], T. Takahashi[2,3], Z. Wang[4], X. Dai[1], Z. Fang[1], G. F. Chen[1], J. L. Luo[1] and N. L. Wang[1]

[1] *Beijing National Laboratory for Condensed Matter Physics, and Institute of Physics, Chinese Academy of Sciences Beijing 100190, China*
[2] *WPI Research Center, Advanced Institute for Material Research, Tohoku University - Sendai 980-8577, Japan*
[3] *Department of Physics, Tohoku University - Sendai 980-8578, Japan*
[4] *Department of Physics, Boston College - Chestnut Hill, MA 02467, USA*

received 3 July 2008; accepted 7 July 2008
published online 14 July 2008

PACS 74.25.Jb – Electronic structure
PACS 74.70.-b – Superconducting materials
PACS 79.60.-i – Photoemission and photoelectron spectra

Abstract – We have performed a high-resolution angle-resolved photoelectron spectroscopy study on the newly discovered superconductor $Ba_{0.6}K_{0.4}Fe_2As_2$ ($T_c = 37\,K$). We have observed two superconducting gaps with different values: a large gap ($\Delta \sim 12\,meV$) on the two small hole-like and electron-like Fermi surface (FS) sheets, and a small gap ($\sim 6\,meV$) on the large hole-like FS. Both gaps, closing simultaneously at the bulk transition temperature (T_c), are nodeless and nearly isotropic around their respective FS sheets. The isotropic pairing interactions are strongly orbital dependent, as the ratio $2\Delta/k_BT_c$ switches from weak to strong coupling on different bands. The same and surprisingly large superconducting gap due to strong pairing on the two small FSs, which are connected by the (π, 0) spin-density-wave vector in the parent compound, strongly suggests that the pairing mechanism originates from the inter-band interactions between these two nested FS sheets.

The recent discovery of superconductivity in iron-arsenic compounds below a transition temperature (T_c) as high as 55 K [1–5] ended the monopoly of copper oxides (cuprates) in the family of high-T_c superconductors. As in the case of cuprates, a critical issue in understanding this new superconductor is the nature and particularly the symmetry and orbital dependence of the superconducting gap. There are conflicting experimental results, mostly from indirect measurements of the low-energy excitation gap, ranging from one gap [6] to two gaps [7,8], from line nodes [8] to nodeless [6,9] gap function in momentum space. In this letter we report a direct observation of the superconducting gap, including its momentum, temperature, and Fermi surface (FS) dependence in $Ba_{0.6}K_{0.4}Fe_2As_2$ ($T_c = 37\,K$) using angle-resolved photoelectron spectroscopy (ARPES).

High-quality single crystals of $Ba_{0.6}K_{0.4}Fe_2As_2$ used in our study were grown by the flux method [10]. High-resolution ARPES measurements were performed in the photoemission laboratory of Tohoku University using a microwave-driven helium source ($h\nu = 21.218\,eV$) with an energy resolution of 2–4 meV and momentum resolution of $0.007\,Å^{-1}$. Samples were cleaved *in situ* at 15 K and measured at 7–50 K in a working vacuum better than 5×10^{-11} torr. Low-energy electron diffraction on a measured surface shows a sharp 1×1 pattern without any detectable reconstruction down to 80 K. A mirror-like sample surface was found to be stable without obvious degradation for the measurement period of 3 days.

Our ARPES measurements in the normal state at $T = 50\,K$ revealed three FS sheets in $Ba_{0.6}K_{0.4}Fe_2As_2$ single crystals. They consist of an inner hole-like FS pocket (from now on we refer to it as the α FS) and an outer hole-like FS sheet (the β FS), both centered at the zone center Γ, and an electron-like FS (the γ FS) centered at M, or (π, 0) defined in the unreconstructed Brillouin zone (BZ). A more accurate FS contour can be traced out from an ARPES intensity plot near the Fermi energy (E_F) at

(a) E-mail: dingh@aphy.iphy.ac.cn

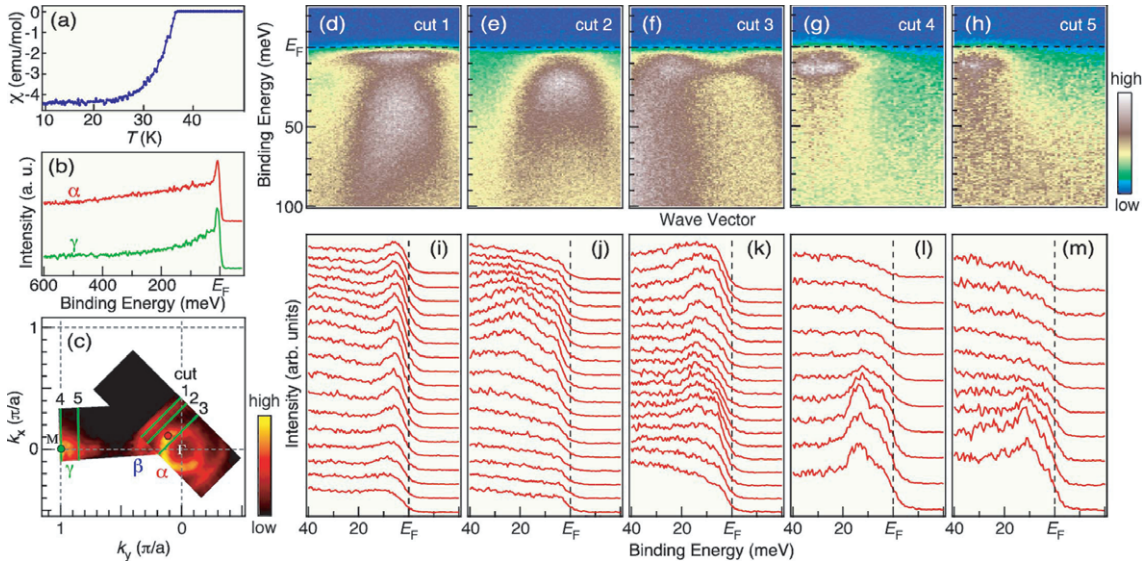

Fig. 1: (Colour on-line) (a) AC susceptibility of $Ba_{0.6}K_{0.4}Fe_2As_2$ ($T_c = 37$ K) as a function of temperature. (b) Representative ARPES spectra in the vicinity of k_F measured in the superconducting state ($T = 15$ K) at two points marked by the circles in the BZ shown in (c). Clear dispersion and sharp QP peaks were observed, indicating good sample (surface) quality. (c) FS contour determined by plotting the ARPES spectral intensity integrated within ±10 meV with respect to E_F. (d)–(h) ARPES spectral intensity at 15 K as a function of wave vector and binding energy. (i)–(m) Corresponding EDCs measured along several cuts in the BZ shown in (c).

low temperatures in the superconducting state, with the help of the sharp quasiparticle (QP) peaks that emerge below T_c in this material as shown in fig. 1(b). The α FS is nearly circular with an enclosed area of $\sim 4\%$ of the reconstructed BZ area. The β FS is more square-like with an area of $\sim 18\%$, and the electron-like γ FS is an ellipse elongated along the Γ-M direction occupying an area of $\sim 3\%$. Thus, according to the Luttinger theorem, the total hole concentration is 38%, close to the nominal bulk hole concentration of 40% per two Fe atoms in a doubled unit cell. The observed FS topology (fig. 1(c)) agrees well with the LDA band theory predictions at $k_z = \pi$. We caution that the k_z dispersion of the β FS and a possible third hole-like pocket of similar size as the α FS, predicted by band calculations [11,12], may affect the carrier counting. When the samples are cooled down below T_c, as shown in the energy distribution curves (EDCs) in figs. 1(i)–(m) at $T = 15$ K, we clearly observe that the leading edge of the spectra on all three FS sheets shifts away from E_F, indicating the opening of an energy gap. In addition, sharp QP peaks are observed in the vicinity of the Fermi crossing (k_F) points, enabling us to estimate the gap values from the QP peak positions. As can be seen in figs. 1(i)–(m), the gap opened on the β FS is clearly smaller than those on the α and γ FS. It is also interesting to note that the spectral linewidth near the β FS is sharper than the ones near the α and γ FS, indicating a longer QP lifetime or reduced scattering rate for the low-energy β band excitations. In fact, the QPs near the α and γ FS have a similar unconventional QP lineshape, with an additional shoulder appearing on the low-energy side of the main QP peak, which will be discussed further below. Comparing to the normal-state dispersion, we find that the QP dispersion (excluding the low-energy shoulder) in the superconducting state reaches a local minimum at k_F with the bending-back effect, similar to the Bogoliubov QP (BQP) dispersion observed in the high-T_c cuprate superconductors [13]. Such a dispersion behavior usually indicates the opening of a superconducting energy gap for the dispersive QPs.

To provide further evidence that the observed gap is indeed the superconducting gap, we have performed temperature (T) dependent measurements along the three cuts displayed in fig. 2, crossing the three FS sheets, respectively. Following a common practice in ARPES [14], we symmetrize the EDCs at k_F to approximately remove the effect of the Fermi function to the leading edge and QP peak position, and extract the full gap (2Δ) from the separation of the two symmetrical QP peaks. Figure 2(b) shows the T-dependence of a symmetrized EDC on the α FS. We clearly observe that the main QP peak position remains at a constant energy (~ 12 meV) from 7 K to 30 K and moves rapidly toward E_F within the narrow temperature range of 35–40 K, accompanied by a sudden broadening of the linewidth. This is very similar to the behavior of the superconducting gap closing at T_c observed in the overdoped high-T_c cuprates [15]. The extracted gap values at different temperatures are plotted in fig. 2(c), which clearly shows that the gap collapses at the bulk T_c at a rate steeper than the classic BCS curve (the red line in fig. 2(c)). Similar T-dependence is also observed for the other two gaps on the β and γ FS sheets, as can be seen in

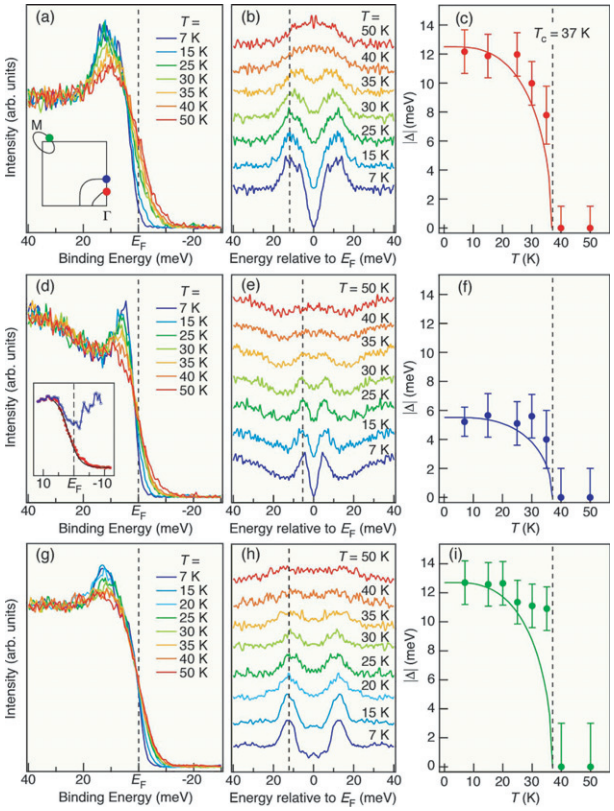

Fig. 2: (Colour on-line) (a) T-dependence of EDC measured at the k_F point of the α FS (red dot in inset). (b) Symmetrized EDCs. The dashed line denotes the position of the QP peak. (c) T-dependence of the superconducting-energy-gap size. The solid line is the BCS mean-field gap equation with $T_c = 37$ K and zero-temperature gap $\Delta(0) = 12.5$ meV. (d)–(f), ((g)–(i)) same as (a)–(c), but measured on the k_F point of the β (γ) FS (blue (green) dots in the inset to (a)). The zero-temperature gap value used in the BCS equation (solid line in (f) and (i)) is $\Delta(0) = 5.5$ and 12.5 meV, respectively. Note that the rapid drop of the gap value on approaching T_c from the superconducting side cannot be described by the BCS mean-field theory. The inset in (d) shows the expansion of the EDC near E_F at 25 K (red), together with the EDC (blue) after dividing out the Fermi function. Nearly particle-hole symmetric BQP peaks are clearly visible, indicating the superconducting nature of the energy gap.

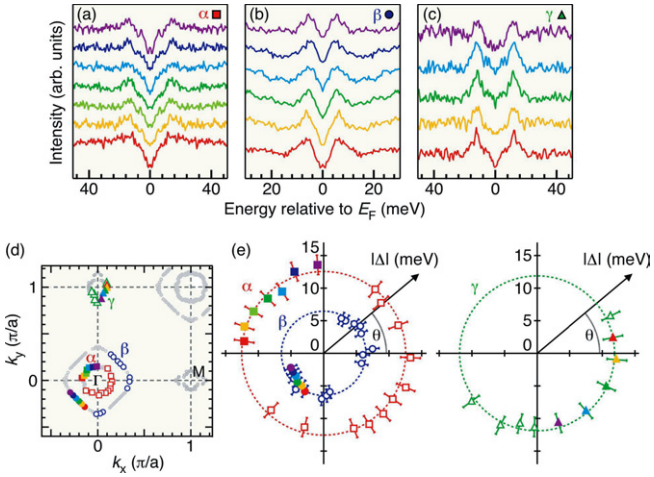

Fig. 3: (Colour on-line) (a)–(c) Symmetrized EDCs at 15 K measured at various k_F points on the α, β, and γ FS, labeled by respective coloured symbols correspondingly. (d) Extracted FS from ARPES measurements in the superconducting state. (e) Superconducting-gap values at 15 K extracted from the EDCs ((a), (b), and (c)) shown on polar plot for the α, β (left) and γ (right) FS as a function the of the FS angle (θ) (zero degree is along Γ-M). A nearly isotropic superconducting gap with weak anisotropy can be seen for all the three observed FS sheets.

figs. 2(d)–(i). In addition, the superconducting spectra can be recovered without any noticeable changes after several thermal cycles up to 50 K. The superconducting nature of these QP gaps are further supported by the observation of a residual BQP hole branch above E_F [16], as shown in the inset of fig. 2(d) for the β FS, where the full spectral function recovered after removing (dividing) the Fermi function shows good particle-hole symmetry, a hallmark associated with the superconducting gap.

We turn to the low-energy shoulder on the spectra of the α and γ FS, which seems to follow a different T-dependence; it broadens rapidly around 15–25 K, which is well below T_c, suggesting a different origin. At $T = 7$ K, this shoulder evolves into a peak structure, but with a strongly sample-dependent location generally within 6 meV of the Fermi level. In contrast, the superconducting gaps along the three FS sheets are robust and sample independent. Although further studies are needed to resolve this issue, we believe that the shoulder features are either due to surface effects or a minority phase that does not superconduct.

By utilizing the momentum-resolving capability of ARPES, we have mapped out the complete superconducting gaps along the three FS sheets. Symmetrized EDCs measured at k_F, some of which are shown in figs. 3(a)–(c), are used to extract the k-dependence of the superconducting gap. It is apparent from viewing these EDCs that the superconducting gaps on the three FS sheets are nearly isotropic with a less-than-20% anisotropy. Figure 3(e) displays the full k-dependence on a polar plot, confirming that nodeless superconducting gaps open on all the FS sheets. The k-averaged gap values are approximately 12, 6, and 12 meV for the α, β, and γ FS, smaller than the superconducting gap of the electron-doped $NdFeAsO_{1-x}F_x$ observed by an earlier ARPES study [17]. This yields the ratio of $2\Delta/k_BT_c$ of 7.5, 3.7, and 7.5, respectively. While the ratio on the β FS is close to the BCS value (3.52), the larger ratio on the α and γ FS, similar to the value observed in many high-T_c cuprates, suggests that pairing is in the strong-coupling regime on these two FS sheets.

We summarize our main results in fig. 4. We have demonstrated the multi-orbital nature of the superconducting state in $Ba_{0.6}K_{0.4}Fe_2As_2$ single crystals, a prototypical hole-doped iron-arsenic superconductor.

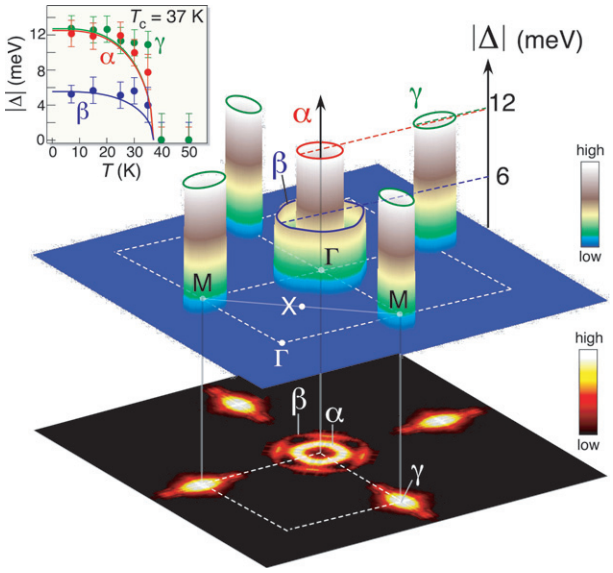

Fig. 4: (Colour on-line) Three-dimensional plot of the superconducting-gap size (Δ) measured at 15 K on the three observed FS sheets (shown at the bottom as an intensity plot) and their temperature evolutions (inset).

Nearly isotropic and nodeless superconducting gaps of different values open simultaneously at the bulk T_c on all three observed FS sheets of electron and hole characters. The most natural interpretation of our findings is that the pairing order parameter has an *s*-wave symmetry, although we cannot rule out the possibility of nontrivial relative phases between the pairing order parameters on the different FS sheets. Perhaps the most striking feature is that strong pairing on the α and γ FS produced nearly the same, surprisingly large superconducting gaps. In the undoped parent compound, these two FS sheets are nested by the $Q = (\pi, 0)$ spin-density-wave (SDW) wave vector [18]. In the sufficiently hole-doped superconducting sample, we have observed evidence of a similar band folding between Γ and M points at low temperatures which could be due to SDW fluctuations or short-range order by the same vector Q. Remarkably, the α and γ FS are still well connected by the Q-vector reminiscent of an inter-band nesting condition along large portions of the two FSs. The latter can enhance the kinetic process where a zero momentum pair formed on the α (γ) FS is scattered onto the γ (α) FS by the fluctuations near the wave vector Q, whereby increasing the pairing amplitude. These observations strongly suggest that the inter-band interactions play an important role in the superconducting pairing mechanism of this new class of high-temperature superconductors.

* * *

This work was supported by grants from the Chinese Academy of Sciences, NSF, Ministry of Science and Technology of China, JSPS, JST-CREST, MEXT of Japan, and NSF, DOE of US.

REFERENCES

[1] Kamihara Y., Watanabe T., Hirano M. and Hosono H., *J. Am. Chem. Soc.*, **130** (2008) 3296.
[2] Wen H. H., Mu G., Fang L., Yang H. and Zhu X. Y., *Europhys. Lett.*, **82** (2008) 17009.
[3] Chen X. H. *et al.*, cond-mat arXiv:0803.3603 (2008).
[4] Chen G. F. *et al.*, *Phys. Rev. Lett.*, **100** (2008) 247002.
[5] Ren Z. A. *et al.*, *Chin. Phys. Lett.*, **25** (2008) 2215.
[6] Chen T. Y. *et al.*, *Nature (London)*, **453** (2008) 1224.
[7] Wang Y. *et al.*, cond-mat arXiv:0806.1986 (2008).
[8] Matano K. *et al.*, cond-mat arXiv:0806.0249 (2008).
[9] Hashimoto K. *et al.*, cond-mat arXiv:0806.3149 (2008).
[10] Chen G. F. *et al.*, cond-mat arXiv:0806.2648 (2008).
[11] Ma F., Lu Z.-Y. and Xiang T., cond-mat arXiv:0806.3526 (2008).
[12] Xu G., Zhang H., Dai X. and Fang Z., cond-mat arXiv:0807.1401 (2008).
[13] Campuzano J. C. *et al.*, *Phys. Rev. B*, **53** (1996) R14737.
[14] Norman M. R. *et al.*, *Nature (London)*, **392** (1998) 157.
[15] Norman M. R., Randeria M., Ding H. and Campuzano J. C., *Phys. Rev. B*, **57** (1998) R11093.
[16] Matsui H. *et al.*, *Phys. Rev. Lett.*, **90** (2003) 217002.
[17] Liu C. *et al.*, cond-mat arXiv:0806.2147 (2008).
[18] Huang Q. *et al.*, cond-mat arXiv:0806.2776 (2008).